Comment on "Exploring Potential Energy Surface with External Forces"

Journal:	*Journal of Chemical Theory and Computation*
Manuscript ID	ct-2019-00736h.R2
Manuscript Type:	Article
Date Submitted by the Author:	n/a
Complete List of Authors:	Quapp, Wolfgang; Universitat Leipzig, Mathematisches Institut Bofill, Josep; Univeridad de Barcelona, Facul. Quimica, Química Inorgànica i Orgànica, secció de Química Orgànica

Comment on "Exploring Potential Energy Surface with External Forces"

Wolfgang Quapp*,† and Josep Maria Bofill*,‡

Mathematisches Institut, Universität Leipzig, PF 100920, D-04009 Leipzig, Germany, and Departament de Química Inorgànica i Orgànica, Universitat de Barcelona, and Institut de Química Teòrica i Computacional, Universitat de Barcelona, (IQTCUB), Martí i Franquès, 1, 08028 Barcelona, Spain

E-mail: quapp@uni-leipzig.de; jmbofill@ub.edu

Abstract

Recently a work (K. Wolinski, J. Chem. Theory Comput. 2018, 14, 6306, DOI: 10.1021/acs.jctc.8b00885) was published in which the SEGO method (Standard and Enforced Geometry Optimization) was proposed to find new minimums on potential energy surfaces. We study this important method from a theoretical point of view. Up to date, the understanding of the proposer does not take into account the barrier breakdown point on a SEGO path being usually half of the path which is searched for. However, a better understanding of the method allows us to follow along the reaction pathway from a minimum to a saddle point, or vice versa. We discuss the well-known two-dimensional MB-test surface where we calculate full SEGO pathways. If one has special SEGO curves at hand, one can also detect some weaknesses of the ansatz.

*To whom correspondence should be addressed
†Leipzig University
‡Universitat de Barcelona

1 Introduction

Considerable interest is attached to the search of reaction pathways in chemistry, especially the points which govern these ways: minimums and saddle points of index one (SP_1) on the potential energy surface (PES) of a reaction system. The reaction pathway is formally defined as a one-dimensional description of a chemical reaction through a sequence of molecular geometries in an N-dimensional configuration space.

The SEGO method is an ansatz which disturbs the given PES by an external force.[1–3] It is a more general case of the special treatments in mechanochemistry.[4–6] It has some similarity with the AFIR method of the Maeda-Morokuma group (artificial force induced reaction).[7] By the external disturbance one moves the stationary points of the former PES to new locations. By following the successive force-displaced stationary points one gets a curve which can, in good cases, connect a minimum and an SP_1 by a kind of reaction path. The SEGO path has an analogous property.

This paper has the following Sections: next we refer to the SEGO method, and we calculate a curve by consecutive SEGO points. A more theoretical tool is obtained for full SEGO curves by a variational formula. A further special property like an avoided crossing is discussed separately, as well as a generalization of the SEGO ansatz, and its dependence on the coordinates. At the end we add a Discussion and a Conclusion.

2 The SEGO Method

The proposal of Wolinski et al. is to use an effective PES[1–3,8,9] with internal coordinates $\mathbf{r}$ of a dimension N

$$V_{eff}(\mathbf{r}) = V(\mathbf{r}) + \frac{1}{2} s \; \mathbf{r}^T \; \mathbf{H}(\mathbf{r}_o) \; \mathbf{r} \; . \tag{1}$$

Here $V(\mathbf{r})$ is the original PES, $\mathbf{H}(\mathbf{r}_o)$ is the Hessian matrix of the second derivatives of the PES at an initial minimum of the PES, at $\mathbf{r}_o$, and s is the important SEGO factor which

plays the role of a numerical parameter driving the calculation. s scales the amount of the force vector. To imagine the external force, $\mathbf{f}$, directly, we write it separately

$$\mathbf{f}(\mathbf{r}) = s\ \mathbf{H}(\mathbf{r}_o)\ \mathbf{r}\ , \tag{2}$$

and the effective PES is

$$V_{eff}(\mathbf{r}) = V(\mathbf{r}) + \frac{1}{2} s\ \mathbf{f}(\mathbf{r})^T \cdot \mathbf{r}\ , \tag{3}$$

with a scalar product where the force, $\mathbf{f}$, acts on the current point, $\mathbf{r}$. In contrast to a general model in Mechanochemistry,[4,10] here the force is not a constant vector. To get a zero force one has to put s=0. Then we have the original PES. The cases with increasing or decreasing s are interesting.

Of course, if the extra force moves all stationary points of the PES out of their former places then a minimum and an SP can coalesce, and a former barrier can disappear. Such a situation is named barrier breakdown point (BBP with $s = s_{max}$), compare it for Newton trajectories (NTs).[11,12] At $s = s_{max}$ a new valley opens for a contact between former distant minimums because the former, initial minimum at $V(\mathbf{r_o})$ disappears, and another minimum of $V_{eff}(\mathbf{r})$ can appear near a searched, next minimum of the original $V(\mathbf{r})$. Thus, one can use the ansatz to detect reaction valleys and new minimums.[3,9,13] The idea is to use an $s > s_{max}$ and to calculate by a large jump a new minimum in the new valley. This is then used as initial value for an optimization of a new minimum on the original PES. One can compare many examples for NTs with pictures of the corresponding effective surfaces.[5,6,10,12,14–16]

We will find here the full SEGO curve between a minimum and an SP_1. To this end, one can start at a known minimum with $s = 0$. Like for NTs,[5,6,17] a continuous increase of the strength of the force, $\pm s$, will move the stationary points of the effective new PES. Of course, every optimization of a stationary point of V_{eff} usually uses the current Hessian. But one can update the Hessian here, and this is no insurmountable difficulty. The original SEGO

method also has to optimize a new minimum after its jump, and one should not update the Hessian for this aim.

We propose to improve the SEGO method by the treatment of two alternating pieces of the curve of new stationary SEGO points. We propose to use an increase of the parameter, s, up to an s_{max} at the BBP of the SEGO curve, and a decrease of the parameter, s, after the BBP. Then the obtained curve points could fully describe the curve between two original stationary points over a BBP, like in the case of NTs.[5] The maximal s-value determines the BBP. Note that the BBP is not an approximation of the original SP of the PES. The BBP is usually anywhere between the initial minimum and the next SP. At the BBP the gradient, $\mathbf{g}(\mathbf{r})$, of the PES, $V(\mathbf{r})$, has a maximal norm, see some instructive discussions[5] for NTs. At the next sought-after stationary point, the parameter s has again to converge to zero.

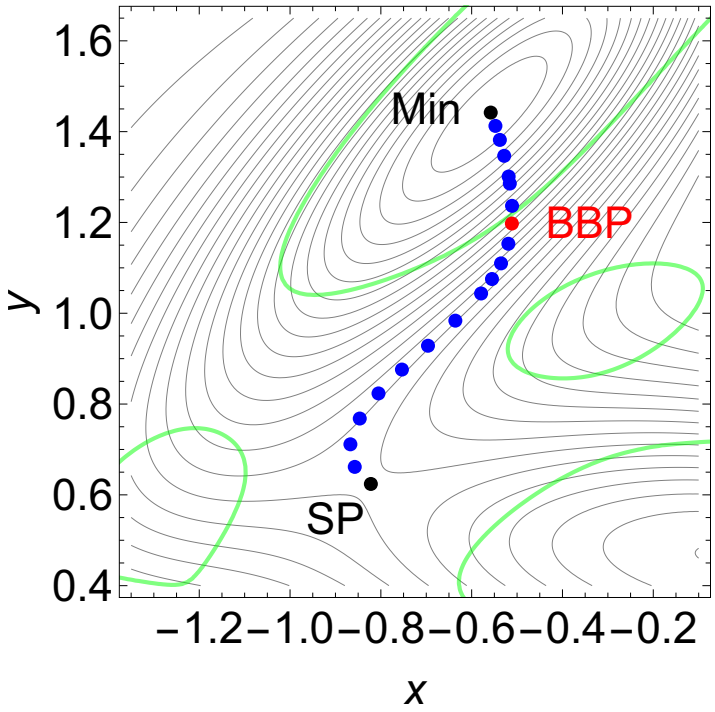

Figure 1: Test surface MB[18] with SEGO points (blue) between the stationary points, the global minimum and the first SP (black points). The level lines are equidistant. The BBP is depicted by a red point; here a curve with $Det(\mathbf{H}) = 0$ (green) crosses the SEGO points.

Figure 1 shows the result of calculations for changing values of s for the Müller-Brown (MB) test surface.[5,18] We use (x, y) for only two abstract coordinates, thus for dimension

N=2. The calculation goes step by step. We put a value of the parameter $s = 0.01$ near zero, and search the next stationary point of the effective PES (1). This point is used for the next s-step as an initial value for the optimization. And so forth. Because the Hessian of the MB surface has very large entries at the global minimum, we have to start with a low $s = 0.01$. With successive 0.005 steps we can go up to $s_{max} = 0.048675$ where the BBP is reached. The exact value of s_{max} can be determined by a trial and error process. One hint is that for a higher s-value no solution exists nearby of an optimization of a curve point. Another hint is to get by calculation of the determinant of the current Hessian which undergoes a sign change here. At s_{max} it holds $Det(\mathbf{H}) = 0$. Thus along the SEGO paths, a possible BBP can be identified by a test of this parameter. After the BBP, to go up to the SP, we again have to decrease the s-parameter.

The procedure to go up by small steps for s and optimize the corresponding stationary point, up to a BBP, and then go back to zero for s to find an SP_1, should work in every dimension N for the SEGO method if no avoided crossing emerges, see below section 4.1.

3 SEGO Curves by a Variational Formula

We use a first variational structure[19] of the SEGO model

$$\mathbf{g}(\mathbf{r}) + s\ \boldsymbol{\varphi}(\mathbf{r}) = \mathbf{0} \tag{4}$$

where $\mathbf{g}(\mathbf{r})$ is the gradient of the PES, s is the Lagrange multiplier and $\boldsymbol{\varphi}(\mathbf{r})$ is the derivation of the extra term, $\boldsymbol{\varphi}(\mathbf{r}) = \nabla_{\mathbf{r}}(\mathbf{f}(\mathbf{r})^T \cdot \mathbf{r})$. If we assume that $\boldsymbol{\varphi}(\mathbf{r}) \neq \mathbf{0}$ we can write the variation ansatz in another form

$$\left(\mathbf{U} - \frac{\boldsymbol{\varphi}(\mathbf{r})\boldsymbol{\varphi}(\mathbf{r})^T}{\boldsymbol{\varphi}(\mathbf{r})^T\boldsymbol{\varphi}(\mathbf{r})}\right)\mathbf{g}(\mathbf{r}) = \mathbf{0} \tag{5}$$

where $\mathbf{U}$ is the unit matrix. If one assumes a continuous SEGO curve by $\mathbf{r}(t)$ with the curve length parameter t then one can derivate Eq.(5) to t to get an implicit equation for

the tangent, $\frac{d\mathbf{r}}{dt}$, of the SEGO curve in Eq.(7), like for NTs.[17] The tangent can be used in a predictor-corrector procedure to effectively calculate the curve without an optimization of the stationary points of the corresponding V_{eff}. The expression can be derived using the directional derivative concept. First we multiplicate Eq. (4) from the left by $\boldsymbol{\varphi}(\mathbf{r})^T$ to obtain an expression for the Lagrange multiplier in the form

$$s(\mathbf{r}) = -\frac{\mathbf{g}^T(\mathbf{r})\,\boldsymbol{\varphi}(\mathbf{r})}{\boldsymbol{\varphi}^T(\mathbf{r})\boldsymbol{\varphi}(\mathbf{r})} \ . \tag{6}$$

With $\mathbf{G}(\mathbf{r}) = \nabla_{\mathbf{r}}\boldsymbol{\varphi}^T(\mathbf{r})$ we obtain with Eqs.(4) and (6)

$$\left[\mathbf{H}(\mathbf{r}) + s(\mathbf{r})\mathbf{G}(\mathbf{r}) + \boldsymbol{\varphi}(\mathbf{r})\nabla_{\mathbf{r}}^T s(\mathbf{r})\right]\frac{d\mathbf{r}}{dt} = \mathbf{0} \ , \tag{7}$$

where $\nabla_{\mathbf{r}} s(\mathbf{r})$ has the form

$$\nabla_{\mathbf{r}}^T s(\mathbf{r}) = -\frac{\mathbf{g}^T(\mathbf{r})}{\boldsymbol{\varphi}^T(\mathbf{r})\boldsymbol{\varphi}(\mathbf{r})}\left[\mathbf{U} - 2\frac{\boldsymbol{\varphi}(\mathbf{r})\boldsymbol{\varphi}^T(\mathbf{r})}{\boldsymbol{\varphi}^T(\mathbf{r})\boldsymbol{\varphi}(\mathbf{r})}\right]\mathbf{G}(\mathbf{r}) - \frac{\boldsymbol{\varphi}^T(\mathbf{r})}{\boldsymbol{\varphi}^T(\mathbf{r})\boldsymbol{\varphi}(\mathbf{r})}\mathbf{H}(\mathbf{r}) \ . \tag{8}$$

May be a problem for Eq.(8) is the quite complicated expression of $\boldsymbol{\varphi}(\mathbf{r})$ for the model ansatz of Eq.(1). For NTs the corresponding tangent equation is quite easier.[17,20]

In the case of $N = 2$, we can use Eq.(5) for a numeric search of a solution of the SEGO curves. We employ a Mathematica contour plot in Figure 2 for the zero contour of the square of the norm of the left hand side of Eq.(5). The point by point optimized SEGO points of Figure 1 fit well in a resulting curve between the reactant minimum, Min_R, and the highest SP of the MB surface, the SP_h.

Note: here emerges a small gap, an avoided crossing, between the intermediate minimum, Min_I, and the rightmost minimum, Min_P.

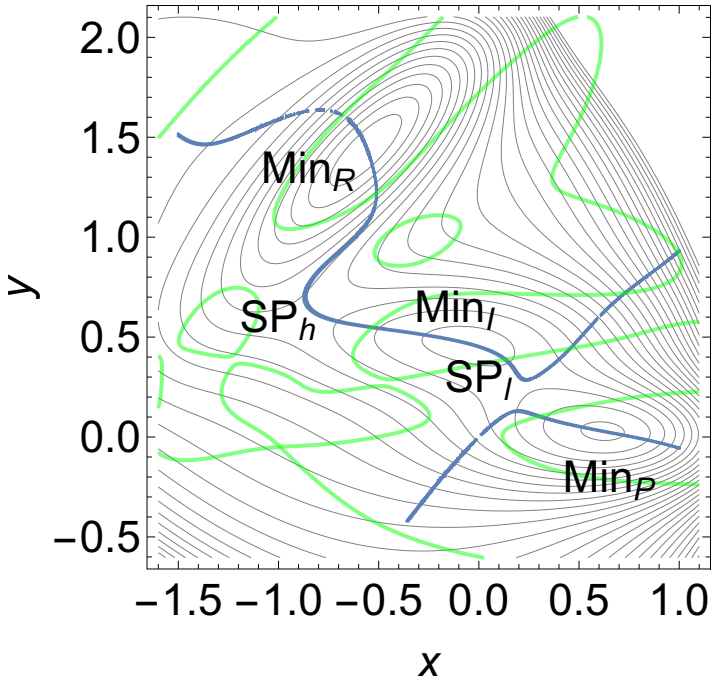

Figure 2: Test surface MB[18] with continuous SEGO curves (blue) through the stationary points. Minimums and SPs are indicated. Curves $Det(\mathbf{H}) = 0$ are depicted in green color. Their crossing with the SEGO curve is the corresponding BBP of this curve. Note an avoided crossing of two SEGO curves between SP_l and Min_P.

4 Some Critical Properties of SEGO Curves

4.1 Avoided Crossing (AC)

A SEGO curve can suffer from an AC. We could not assign any useful property of the PES to such ACs. It is in contrast to NTs. There the ACs indicate the neighborhood of a valley-ridge inflection (VRI) point which is crossed by a bifurcating, a singular NT.[20] Singular NTs divide the 'regions of influence' of the different stationary points. However here, so to say, 'singular' SEGO curves with a bifurcation are very seldom because these curves do not form a dense family of curves. At first view, they are unique curves, compare the next subsection 4.2. With the given definition, one cannot try to change the 'search-direction' of the SEGO curve to get a nearby 'singular' SEGO curve like a singular NT. The bifurcation of NTs is quite easier to calculate[21] and it directly depends on the Hessian of the PES. Because of the nonlinearity of ansatz (1) the connection to the Hessian will be quite more complicated for

SEGO.

The action of an AC can be dramatically, but must not. In our example of the MB surface and with the SEGO curve of Figure 2, we show this for the current effective PES for parameter $s_{max} = 0.048675$. In Figure 3 (a) we can show the coalescence of the global minimum and the highest SP into a shoulder (Sh). The former global minimum bowl is tipped over. The reactant would 'flow' into the new global minimum, Min_P. If one has calculated this minimum, one can use it for a calculation of the true Min_P of the original PES. The intermediate, Min_I, already disappeared earlier at the local $s_{max} = 0.031$. Min_I coalesces with the former SP_l to a shoulder on the upper branch of the SEGO curve.

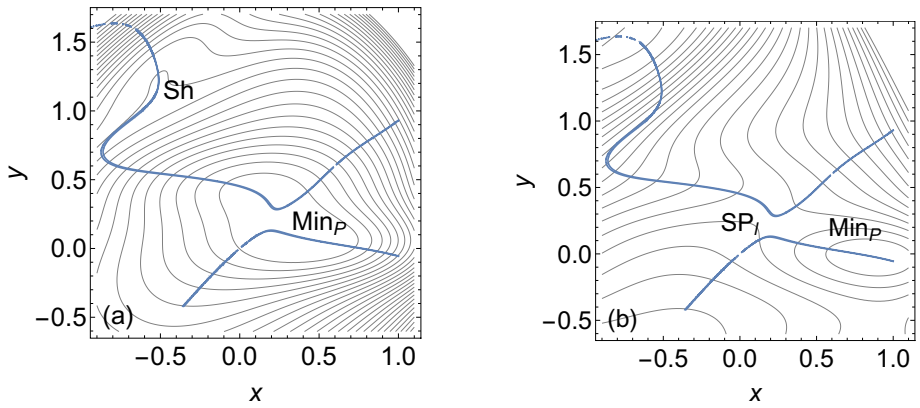

Figure 3: (a) Effective MB surface of Eq.(1) with $s = 0.48675$. Sh is the shoulder. The V_{eff} can be used to calculate the product minimum, Min_P by steepest descent starting in Min_R. The SEGO curves are further depicted in blue and they are included. (b) The effective MB surface of Eq.(1) with $s = -0.48675$. Here the SP_l survived, and the SEGO curve does not lead along a simple valley.

In contrast, in Figure 3 (b) we use the inverse tipping by $s = -0.048675$. Now the barrier between the intermediate and the global minimum disappears again, but the former barrier SP_l survives. Min_I and the former SP_h disappear. SP_l also survives for still higher values of the parameter, s. This means that a calculation starting in Min_P does not 'flow' back to the former Min_R. For the task the SEGO method would not work: an AC can prohibit SEGO. The corresponding stationary points, Min_P and SP_l, cannot coalesce because on the separated curves.

4.2 The Fixing of the Force Direction by $\mathbf{H}(\mathbf{r}_0)$

With the force (2) at the initial minimum, the SEGO curve will usually not be directed into an eigenvector direction of the Hessian, one can compare Figures 1 and 2 where the SEGO curve starts in any direction in between the eigenvectors of the global minimum. (The eigenvectors of the Hessian at the global minimum are the main axes of the ellipse of the first level line.) If it was the intention of the author in Ref.[3] to use an eigenvector direction of the initial Hessian then the ansatz of Eq. (1) is not correct. The force (2) is a rotation of the accidental coordinate direction $\mathbf{r_o}$ by the Hessian. Only if the coordinate $\mathbf{r_o}$ points accidentally itself into the direction of an eigenvector, then the SEGO curve starts into such a direction.

In contrast, the action of the Hessian at a minimum is that the corresponding SEGO curve will be turned near to the eigenvector to the largest eigenvalue. That is usually a direction which points into the 'mountains' of the PES, but not to a low lying SP. Thus, the use of the Hessian in definition (2) is more or less pointless, or counterproductive. Any other symmetric matrix will also start a modified SEGO curve, or one can define another SEGO curve by the force $s\ \mathbf{r}$, compare Figure 4 (a).

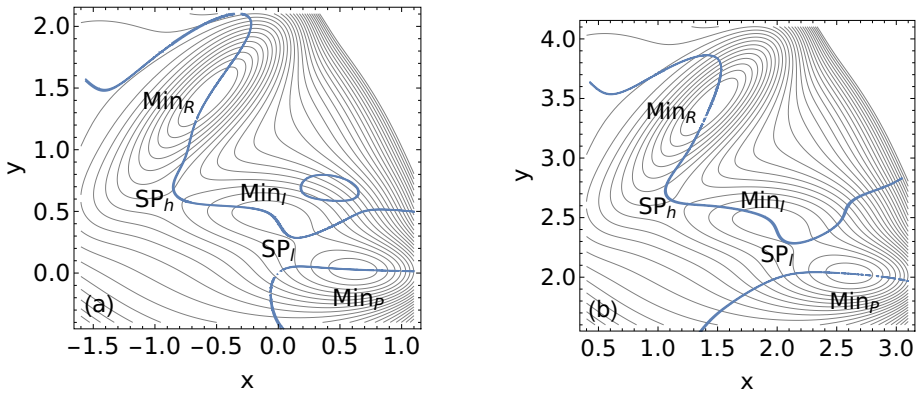

Figure 4: (a) MB surface[18] with modified SEGO curves (blue). The matrix $\mathbf{H}(\mathbf{r}_0)$ of the original SEGO definition in Eq. (2) is substituted by the unit matrix. (b) The same MB surface where all coordinates are symmetrically moved by $(2, 2)$. Then the original SEGO curves also change.

SEGO works because around every stationary point the gradient of the PES rotates a

full 'circle'. So, any force direction can be put against the gradient of the PES to define an external force. For an NT we use a fixed direction, but SEGO uses the variable direction caused by the coordinates, $\mathbf{r}$. Thus it is not surprising that SEGO is a little more complicated than NTs.

If one whishes to start a SEGO curve into an eigenvector direction of the initial Hessian at $\mathbf{r}_o$ then one has to use directly this eigenvector. The matrix $\mathbf{H}(\mathbf{r}_o)$ in Eq.(1) is to replace by the directional matrix $\mathbf{D} = \mathbf{l}\mathbf{l}^T$ with the dyadic product of the used vector, $\mathbf{l}(\mathbf{r}_o)$. Of course one can use in matrix $\mathbf{D}$ any direction. In Fig. 5 we draw the modified SEGO curves to the two eigenvectors at the global minimum of the MB surface. The curves are calculated with the variational formula Eq. (5). The modified SEGO curve to the valley eigenvector follows this valley and does not find the high SP which leads into a side valley. One should count this for a correct behaviour. The SP, on the other hand, is passed by a second branch of a modified SEGO curve to the first eigenvector (again in brown color) because every stationary point is crossed by such a SEGO curve.

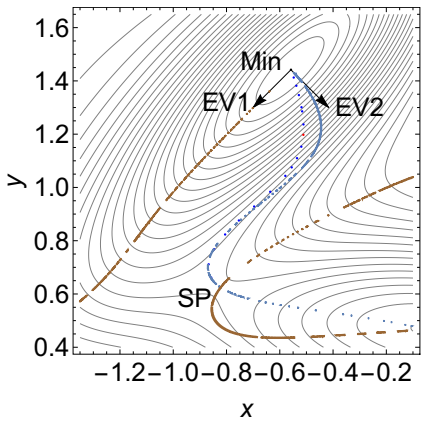

Figure 5: MB surface[18] with modified SEGO curves to the dyadic matrix $\mathbf{D}$, see text. The brown curve is to direction of the first eigenvector along the valley floor of the global minimum. The blue curve starts with eigenvector 2. For comparison the points of Fig. 1 are included.

4.3 Coordinate Dependence of SEGO Curves

Because of the nonlinearity of the SEGO ansatz, Eq.(1), the resulting curves do not only depend on the PES, however, they also depend on the used coordinates. We demonstrate this with a simple coordinate transformation, a movement of (x, y) by $(2, 2)$. The SEGO curves in Figure 4(b) also connect the minimums and the SP_1, but they are a bit changed against the original curves in Figure 2.

5 Discussion

The example demonstrates that the SEGO method can follow a valley from a minimum to an SP_1, or vice versa, at least in good cases.

There are some specific issues that need to be taken into account:

(i) There can be a gap by an avoided crossing of a SEGO curve. The hypothetical bifurcation point inside an avoided crossing seems to have no geometrical meaning. In contrast, regular NTs connect the minimums with the SP_1 of the PES.[22] It is named the index theorem of NTs. Bifurcation points of NTs are valley-ridge inflection points. Note that ACs of SEGO curves can destroy the planed action of the SEGO method.

(ii) The SEGO curve can have a turning point. It means that the curve touches a level line. Such behavior is also known for NTs. If a turning point emerges then the corresponding curve should not be used as a model of a reaction path since the TP can have a higher energy than the next SP_1.

(iii) One SEGO curve leads through every stationary point, correspondingly, to positive or negative values of the parameter, s. It is again like for NTs, but there we can chose any direction which then is the leading direction of the NT. The NTs have a quite greater variability because around a stationary point all search directions are possible – of course also the eigenvector directions of the Hessian are possible. The NTs form a dense net of curves on the PES. And the NTs are a linear ansatz, thus easier to handle than the SEGO

method. NTs are the general solution curves for the force displaced stationary points of the mechanochemical model.

(iv) A search for optimal BBPs[23] is probably possible with generalized SEGO curves if the rotation matrix in force (2) becomes free. To determine an optimal BBP, that means a minimal s_{max}, one needs a continuously changeable direction of the SEGO curve.

(v) In Refs.[1,3,8,24,25] the authors start with the usual ansatz of a mechanochemical model with a constant force vector. Meanwhile we know that the curves of the force-displaced stationary points of this model are the NTs.[6,26] They are well adapted curves towards many problems. However, why does the author[3] go the step from the simple, linear model to the nonlinear model of Eq.(1)? We cannot see the advantages of the more complicated ansatz.

(vi) On the other hand, however, the SEGO model[3] is close to the application of an external electric field to a molecular system, which may be the next step to be studied. In fact, if we take

$$V_{eff}(\mathbf{r}) = V(\mathbf{r}) + V_e(\mathbf{r})$$

where V_e is the external electric field potential given by $V_e(\mathbf{r}) = \mu(\mathbf{r})^T \mathbf{f}_e$ with $\mathbf{f}_e$ is the external electric field of constant direction and $\mu(\mathbf{r})$ is the dipole moment of the molecule. Then, by the same procedure we can write for the force-displaced stationary points

$$\mathbf{g}_{eff}(\mathbf{r}) = \mathbf{0} = \mathbf{g}(\mathbf{r}) + [\nabla_{\mathbf{r}} \mu^T(\mathbf{r})]\mathbf{f}_e \ .$$

Here again emerges the question, is there an optimal $\mathbf{f}_e$?

6 Conclusions

In former applications the SEGO method is handled as a 'black box'. The meaning and the importance of the SEGO parameter, s_{max}, at the BBP for the success of the method

is not discussed. The use of only a fixed value of the parameter, s, for a test calculation[3] where then one hopes to find a next minimum, gives away possibilities of this ansatz. In good cases, a consecutive use of small s-steps can directly follow a reaction path up to the searched SP_1. But one has to be careful: s has to increase up to a 'barrier breakdown point' BBP with $Det(\mathbf{H}) = 0$, and then one has to decrease s back to zero at the next stationary point.

However, the emergence of 'avoided crossings' of SEGO curves can destroy their exploitability for a full reaction pathway.

Overall, we propose to use the simpler and better adapted Newton trajectories, thus a fixed, constant force, $\mathbf{f}$, in Eq. (3).

Acknowledgment

Financial support from the Spanish Ministerio de Economía y Competitividad, Project CTQ2016-76423-P, Spanish Structures of Excellence María de Maeztu program through grant MDM-2017-0767 and from the Generalitat de Catalunya, Departament d'Empresa i Coneixement, Project 2017 SGR 348 is fully acknowledged.

References

(1) Wolinski, K.; Baker, J. Theoretical predictions of enforced structural changes in molecules. *Molec. Phys.* **2009**, *107*, 2403 –2417.

(2) Wolinski, K.; Baker, J. Geometry optimization in the presence of external forces: a theoretical model for enforced structural changes in molecules. *Molec. Phys.* **2010**, *108*, 1845–1856.

(3) Wolinski, K. Exploring Potential Energy Surface with external forces. *J. Chem. Theo. Computat.* **2018**, *14*, 6306 –6316.

(4) Ribas-Ariño, J.; Marx, D. Covalent Mechanochemistry: Theoretical Concepts and Computational Tools with Applications to Molecular Nanomechanics. *Chem. Rev.* **2012**, *112*, 5412–5487.

(5) Quapp, W.; Bofill, J. M. Reaction Rates in a Theory of Mechanochemical Pathways. *J. Comput. Chem.* **2016**, *37*, 2467–2478.

(6) Quapp, W.; Bofill, J. M.; Ribas-Ariño, J. Towards a Theory of Mechanochemistry, Simple Models from the Very Beginnings. *Int. J. Quantum Chem.* **2018**, *118*, e25775.

(7) Maeda, S.; Harabuchi, Y.; Takagi, M.; Saita, K.; Suzuki, K.; Ichino, T.; Sumiya, Y.; Sugiyama, K.; Ono, Y. Implementation and Performance of the Artificial Force Induced Reaction method in the GRRM17 program. *J. Computat. Chem.* **2018**, *39*, 233–250.

(8) Brzyska, A.; Wolinski, K. Enforced conformational changes in the structural units of glycosaminoglycan (non-sulfated heparinbased oligosaccharides). *RSC Adv.* **2014**, *4*, 36640.

(9) Brzyska, A.; Wolinski, K. Isomerization and decomposition of 2-methylfuran with external forces. *J. Chem. Theory Model.* **2019**, *xx*, 1 – 10.

(10) Quapp, W.; Bofill, J. M.; Ribas-Ariño, J. Analysis of the Acting Forces in a Theory of Catalysis and Mechanochemistry. *J. Phys. Chem. A* **2017**, *121*, 2820–2838.

(11) Konda, S. S. M.; Avdoshenko, S. M.; Makarov, D. E. Exploring the Topography of the stress-modified Energy Landscapes of mechanosensitive Molecules. *J. Chem. Phys* **2014**, *140*, 104114.

(12) Quapp, W.; Bofill, J. M. A contribution to a theory of mechanochemical pathways by means of Newton trajectories. *Theoret. Chem. Acc.* **2016**, *135*, 113–132.

(13) Wolinski, K.; Brzyska, A. Theoretical studies of the pyranose ring under mechanical stress. *Carbohydrate Research* **2018**, *470*, 64–72.

(14) Quapp, W.; Bofill, J. M. Mechanochemistry on the Müller-Brown Surface by Newton Trajectories. *Int. J. Quantum Chem.* **2018**, *118*, e25522.

(15) Quapp, W. A Minimal 2D Model of the Free Energy Surface for a Unidirectional Natural Molecular Motor. *J. Math. Chem.* **2018**, *56*, 1339–1347.

(16) Quapp, W.; Bofill, J. M. Newton Trajectories for the Frenkel-Kontorova model. *Molec. Phys.* **2019**, *117*, 1541–1558.

(17) Quapp, W.; Hirsch, M.; Imig, O.; Heidrich, D. Searching for Saddle Points of Potential Energy Surfaces by Following a Reduced Gradient. *J. Comput. Chem.* **1998**, *19*, 1087–1100.

(18) Müller, K.; Brown, L. Location of Saddle Points and Minimum Energy Paths by a Constrained Simplex Optimisation Procedure. *Theor. Chim. Acta* **1979**, *53*, 75–93.

(19) Bofill, J. M.; Quapp, W. Calculus of Variations as a basic Tool for Modeling of Reaction Paths and Localization of Stationary Points on Potential Energy Surfaces. *Molec. Phys.* **2019**, *doi 10.1080/00268976.2019.1667035*.

(20) Quapp, W.; Hirsch, M.; Heidrich, D. Bifurcation of Reaction Pathways: the Set of Valley Ridge Inflection Points of a Simple Three-dimensional Potential Energy Surface. *Theor. Chem. Acc.* **1998**, *100*, 285–299.

(21) Quapp, W.; Hirsch, M.; Heidrich, D. An Approach to Reaction Path Branching using Valley-Ridge-Inflection Points of Potential Energy Surfaces. *Theor. Chem. Acc.* **2004**, *112*, 40–51.

(22) Hirsch, M.; Quapp, W. Reaction Channels of the Potential Energy Surface: Application of Newton Trajectories. *J. Molec. Struct., THEOCHEM* **2004**, *683*, 1–13.

(23) Bofill, J. M.; Ribas-Ariño, J.; García, S. P.; Quapp, W. An Algorithm to Locate Optimal Bond Breaking Points on a Potential Energy Surface. *J.Chem.Phys.* **2017**, *147*, 152710.

(24) Baker, J.; Wolinski, K. Isomerization of Stilbene Using Enforced Geometry Optimization. *J. Computat. Chem.* **2011**, *32*, 43–53.

(25) Baker, J.; Wolinski, K. Kinetically stable high-energy isomers of C14H12 and C12H10N2 derived from cis-stilbene and cis-azobenzene. *J. Mol. Model.* **2011**, *17*, 1335 –1342.

(26) Quapp, W.; Bofill, J. M. Pathways of most Mechanochemical Transformations are Newton Trajectories. *J. Phys. Chem. B* **2016**, *120*, 2644–2645.

TOC Graphics

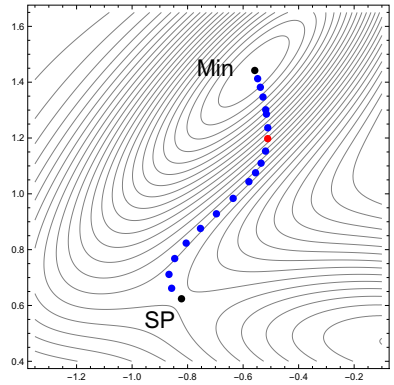

SEGO points on a 2D surface are blue. In black is drawn the global minimum and the next saddle of index one. The red point depicts the maximum of the SEGO-parameter.